frontiers in Marine Science

ORIGINAL RESEARCH
published: 30 August 2021
doi: 10.3389/fmars.2021.699528

Ecoengineering Solutions for the Impairment of Spreading and Growth of Invasive *Spartina patens* in Mediterranean Salt Marshes

Ricardo Cruz de Carvalho[1,2], Eduardo Feijão[1], Irina Duarte[1], Vanessa Pinto[1], Marisa Silva[1], Ana Rita Matos[3,4], Anabela Bernardes da Silva[3,4], Isabel Caçador[1,3], Patrick Reis-Santos[1,5], Vanessa F. Fonseca[1,6] and Bernardo Duarte[1,3]*

[1] *MARE – Marine and Environmental Sciences Centre, Faculdade de Ciências da Universidade de Lisboa, Lisbon, Portugal,* [2] *cE3c – Centre for Ecology, Evolution and Environmental Changes, Faculdade de Ciências da Universidade de Lisboa, Lisbon, Portugal,* [3] *Departamento de Biologia Vegetal, Faculdade de Ciências, Universidade de Lisboa, Lisbon, Portugal,* [4] *Biosystems and Applied Sciences Institute, Faculdade de Ciências da Universidade de Lisboa, Lisbon, Portugal,* [5] *Southern Seas Ecology Laboratories, School of Biological Sciences, The University of Adelaide, Adelaide, SA, Australia,* [6] *Departamento de Biologia Animal da Faculdade de Ciências da Universidade de Lisboa, Lisbon, Portugal*

OPEN ACCESS

Edited by:
Stelios Katsanevakis, University of the Aegean, Greece

Reviewed by:
César Costa, Federal University of Rio Grande, Brazil
Jenneke Visser, University of Louisiana at Lafayette, United States

***Correspondence:**
Ricardo Cruz de Carvalho
rfcruz@fc.ul.pt

Specialty section:
This article was submitted to Marine Ecosystem Ecology, a section of the journal Frontiers in Marine Science

Received: *23 April 2021*
Accepted: *09 August 2021*
Published: *30 August 2021*

Citation:
Cruz de Carvalho R, Feijão E, Duarte I, Pinto V, Silva M, Matos AR, da Silva AB, Caçador I, Reis-Santos P, Fonseca VF and Duarte B (2021) Ecoengineering Solutions for the Impairment of Spreading and Growth of Invasive Spartina patens in Mediterranean Salt Marshes. Front. Mar. Sci. 8:699528. doi: 10.3389/fmars.2021.699528

The invasion of natural communities by non-indigenous species represents one of the most serious threats to biodiversity. Understanding the ecophysiology of invasive species can provide insights into potential physiological handicaps relative to native species. By doing so, we can leverage the development of ecoengineering solutions for the removal of non-indigenous species, preferably using non-chemical methods. *Spartina patens* is a known invasive species of cordgrass aggressively proliferating in Mediterranean salt marshes, producing impenetrable monospecific stands. As its occurrence is delimited by the upper high tide water level, we hypothesized that *S. patens* is intolerant to waterlogging. Therefore, we developed a field experiment where strands of *S. patens* were kept waterlogged over the entire tidal cycle for 30 days. At the end of the experimental period, plants in the trial plots exhibited severe stress symptoms at different physiological levels compared with control plots (no intervention). At the photobiological level, intervened plants exhibited lower efficiency in producing chemical energy from light, whilst at the biochemical level waterlogging impaired the antioxidant system and increased lipid peroxidation products. Furthermore, the application of chlorophyll *a* pulse amplitude modulated (PAM) fluorometry, a non-invasive technique, allowed us to evaluate the effectiveness of the implemented measures, being the tool that provided the best separation between the control and intervened population. Considering the physiological traits observed here, ecoengineering solutions

based on increased waterlogging of *S. patens* stands, can be a low-cost and efficient measure to reduce the spreading and growth of this invasive species in the Mediterranean and other salt marshes worldwide with little disturbance.

Keywords: ecological restoration, invasive species, salt marsh, remote sensing, halophytes

INTRODUCTION

Salt marshes provide a wide range of ecological services, including nursery habitats for many animals, protection against coastal erosion, water purification, having the considerable capacity to store and sequester carbon, and are key players in the ecosystem natural remediation capacity (Couto et al., 2013; Teixeira et al., 2014; Duarte et al., 2018, 2021), being these services valuated in several millions of euros per year (Duarte et al., 2021). Being preferred locations for human settlement and a profusion of anthropogenic activities, coastal, and transitional areas have been severely impacted in their health and functioning worldwide. Habitat loss and degradation, climate change and the introduction of invasive species are amongst the major threats to salt marsh ecosystems (Duarte et al., 2015, 2018; Repolho et al., 2017; Pérez-Romero et al., 2018). Therefore, in the context of increasing degradation rates, the need to restore salt marsh ecosystems has been recognized as a priority by managers, scientists, and general society. This is well-emphasized in the EU Biodiversity Strategy for 2030 and its EU Nature Restoration Plan (EU, 2020) and reinforced by the UN Decade on Ecosystem Restoration (UN, 2020).

Salt marshes have been widely affected by non-indigenous species (NIS) being a serious threat to wetland biodiversity (Heywood, 1989). Although many NIS plants were introduced long ago (more than a century), recent arrivals are of much concern (Aguiar and Ferreira, 2013; Ainouche and Gray, 2016; Martínez-Jauregui et al., 2018). The *Spartina* genus is highly successful amongst the halophyte plant group, being widespread across the globe. These plants have C4-type photosynthesis, in which a CO_2 concentration mechanism at ribulose-1,5-bisphosphate carboxylase-oxygenase (Rubisco) level, involving the fixation of atmospheric CO_2 by phosphoenol-pyruvate carboxylase (PEPC), increases Rubisco carboxylase activity and allows a faster growth rate (von Caemmerer, 2020). *Spartina patens* (Ait.) Muhl. (Gramineae) is a perennial grass distributed along a wide range of coastal habitats, aggressively competing with native species (Duarte et al., 2015). It was introduced in the Mediterranean Sea probably due to ship traffic from America, being used as packing material in ships boxes and crates (Hultén, 1958). Therefore, although being present for some time along the Western Mediterranean coasts, it had not been recorded on the Eastern Iberian coast until recently (Baumel et al., 2016).

Controlling invasive species is relevant for restoration efforts, and several approaches have been developed to address this issue, ranging from herbicide application to mowing and physical removal (Kerr et al., 2016). While the first appears as a simple and cost-effective method (Major et al., 2003; Patten et al., 2017), the long-term effects of herbicides may have serious impacts on the ecosystem (Cruz de Carvalho et al., 2020b). As for the other two methods, they will only prevent further spread needing to be constantly applied and being very time- and cost-consuming (Hedge et al., 2003). Therefore, we considered an alternative method underpinned on the physiology of the species, in particular the fact that *S. patens* has a low tolerance to waterlogging, due to poor aeration of the rhizosphere which consequently impairs its growth (Burdick, 1989; Bertness, 1991; Curado et al., 2020), and naturally limits this species distribution to the high tide border of salt marshes. Thus, in the present work, we tested the application of a physical barrier that would prolong waterlogging around the plants and evaluated the impact on its physiology.

MATERIALS AND METHODS

Plant Material and Collection Site

Sampling occurred before the start of the growing season (February 2020) in the Hortas salt marsh (Alcochete; 38° 45.661' N, 8° 56.116' W), located in the middle estuary, adjacent to the Tagus Estuary Natural Reserve (**Figure 1**). This salt marsh is flooded twice per day, being dominated by the halophyte species *Spartina maritima* in the lower marsh (*circa* 12% coverage), *Halimione portulacoides* in the mid-upper marsh (*circa* 35% coverage), and *Sarcocornia fruticosa* in the upper marsh (*circa* 20% coverage) (Caçador et al., 2013). More recently, the halophyte invasive species *S. patens* has managed to establish itself in the margins, justifying the importance of the current study.

Applied Treatments

Spartina patens plants were subjected to two treatments: (1) control, where the plants did not undergo any intervention, and (2) the waterlogging treatment (waterlogged) where plant turfs filled the inside of a 50 cm long and 10 cm diameter PVC tube buried down into the sediments, leaving an 8 cm margin outside, which allowed the tidal water to enter the tube and remain longer inside and, thus, increase the waterlogging of the plants (n = 5 for each treatment). The experiment lasted for 30 days. Several

Abbreviations: APx, ascorbate peroxidase; CAP, canonical analysis of principal coordinates; CAT, catalase; DBI, double bond index; DTT, dithiothreitol; EDTA, ethylenediaminetetraacetic acid; ETC, electron transport chain; FAME, fatty acids methyl esters; GOPx, guaiacol peroxidase; GR, glutathione reductase; LC-PUFA, polyunsaturated fatty acids; MDA, malondialdehyde; NIS, non-indigenous species; PAM, pulse amplitude modulated; PCO, principal coordinates analysis; PEP, phosphoenol-pyruvate; PEPC, phosphoenol-pyruvate carboxylase; PMSF, phenylmethylsulfonyl fluoride; PS I, photosystem I; PS II, photosystem II; PVC, polyvinyl chloride; PVP, polyvinylpyrrolidone; RC, reaction centers; ROS, reactive oxygen species; Rubisco, ribulose-1,5-bisphosphate carboxylase-oxygenase; SOD, superoxide dismutase; TBA, thiobarbituric acid; TCA, trichloroacetic acid; TPF, triphenyl formazan; TTC, triphenyl-tetrazolium chloride.

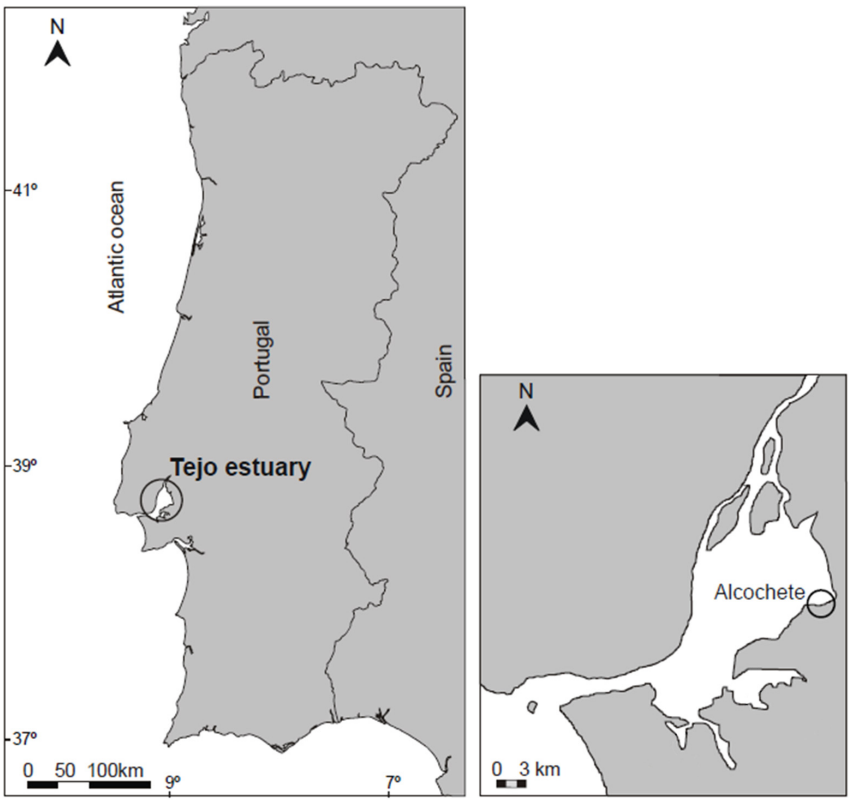

FIGURE 1 | Map of the location of the sampling site in the Hortas salt marsh (Alcochete) in the Tagus estuary.

field measurements were made, namely, *in vivo* chlorophyll *a* pulse amplitude modulated (PAM) fluorometry measurements. Moreover, 20 leaves from each treatment were also collected directly into individual tubes with liquid nitrogen (see sections below). Finally, whole plants of *S. patens* from both treatments were also collected, transported to the lab, washed, removed from excess water, weighted (fresh weight), and oven-dried at 60°C to constant weight (dry weight).

Chlorophyll *a* Pulse Amplitude Modulated Fluorometry

Ten leaves from plants from each treatment were dark-adapted for 15 min and PAM measurements were performed using a FluoroPen FP100 (Photo System Instruments, Czechia). For the analysis of chlorophyll transient light curves (Kautsky plot), and the derived fluorometric parameters (**Table 1**), the JIP-test was used (Duarte et al., 2017).

Leaf Infrared Thermography

Thermal images were obtained with a FLIR E50bx infrared camera (FLIR Systems, Inc., Wilsonville, OR, United States) producing images of 320 × 240 resolution with an accuracy of ±0.045°C. Ten leaves were randomly selected from plants of both treatments, having a water bottle at ambient temperature near the leaves as reference. The average temperature of each leaf was calculated on each image. All image processing and analysis were performed in FLIR Tools software (version 6.4.18039.1003, FLIR Systems, Inc.).

Root Respiration

Fresh fine roots of each treatment weighing approximately 100 mg were transferred to 10-mL reaction tubes, and 6 mL of TTC-solution [0.6% (w/v) triphenyl-tetrazolium chloride in 0.06 M Na_2HPO_4–KH_2PO_4 and 0.05% (v/v) Tween 20] was added to each tube (n = 5) (Brunner et al., 2002). In duplicate tubes, 0.15 mM KCN was added to determine the inhibited respiration. The samples were then incubated for 24 h at 25°C. After incubation, the TTC solution was decanted and triphenyl formazan (TPF) extraction was made by adding 2 mL of ethanol and boiling at 80°C for 15 min (Ruf and Brunner, 2003). After collecting the supernatant in new tubes, the absorbance of 1 mL was measured at 520 nm with a spectrophotometer (UV500 UV-Visible Spectrometer, Unicam, Waltham, MA, United States). The root residues in the test tubes were dried at 80°C for 72 h and weighed. Reduction of TTC was calculated as μg of TPF produced per hour per g dry weight (DW).

Proline Quantification

Proline content was determined according to Bates et al. (1973). For each treatment, plant leaves (n = 5) were homogenized in 3% aqueous sulfosalicylic acid and the homogenate centrifuged a 9,000 g for 15 min at 0°C (Sigma

TABLE 1 | Fluorometric analysis parameters and their description.

JIP-test	
Area	Corresponds to the oxidized quinone pool size available for reduction and is a function of the area above the Kautsky plot
N	Reaction center turnover rate
S_M	Corresponds to the energy needed to close all reaction centers
M_0	Net rate of PS II RC closure
γ_{RC}	Probability that a PS II chlorophyll molecule function as a RC
Ψ_{Eo}	Probability that an absorbed photon will move an electron into the ETC
φ_0	Probability that a trapped excitation moves an electron into the ETC beyond QA
δ_{Ro}	Efficiency of the transfer of an electron from PQH_2 to final PS I acceptors
RE_0/RC	Flux of electrons transferred from PQH_2 to final PSI acceptors per active PS II
ABS/CS	Absorbed energy flux per cross-section
TR_0/CS	Trapped energy flux per cross-section
ET_0/CS	Electron transport energy flux per cross-section
DI_0/CS	Dissipated energy flux per cross-section
RC/CS	Number of available reaction centers per cross-section
P_G	Grouping probability of the connectivity between the two PS II units
$\delta_{Ro}/(1\text{-}\delta_{Ro})$	Contribution of PSI, reducing its end acceptors
$\Psi_0/(1\text{-}\Psi_0)$	Contribution of the dark reactions from Q_A^- to PC
$\Psi_{Eo}/(1\text{-}\Psi_{Eo})$	Equilibrium constant for the redox reactions between PS II and PS I
RC/ABS	Reaction center II density within the antenna chlorophyll bed of PS II
TR_0/DI_0	Contribution or partial performance due to the light reactions for primary photochemistry
SFI	Structure functional index for photosynthesis
SFI (NO)	Non-photosynthetic or dissipation structure functional index

2-16K, SIGMA Laborzentrifugen GmbH, Osterode am Harz, Germany). The supernatant was collected, and the reaction consisted of 2 mL of extract combined with 2 mL of glacial acetic acid and 2 mL of acid ninhydrin. The reaction occurred for 1 h at 100°C, after which the reaction was stopped in an ice bath. The reaction mixture was extracted with 4 mL of toluene and its absorbance read at 520 nm with a spectrophotometer (UV500 UV-Visible Spectrometer, Unicam, Waltham, MA, United States) and compared with a standard curve of proline, expressed in $\mu mol\ g^{-1}$ fresh weight (FW).

C4-Photosynthetic Carboxylating Enzymes Activity and Pigment Analysis

Carboxylating enzymes, PEPC and Rubisco, were extracted from frozen leaf samples according to Carmo-Silva et al. (2008), except that 50 mM HEPES-KOH pH 7.3 was used and 0.5% (v/v) Triton X-100 added. Briefly, approximately 50 mg FW were extracted in a cold mortar containing quartz sand, 1% (w/v) insoluble polyvinylpyrrolidone (PVP) and 1 mL of ice-cold extraction medium [50 mM HEPES-KOH pH 7.3, 1 mM EDTA, 5% (w/v) PVP25000, 6% (w/v) polyethylene glycol (PEG4000), 10 mM dithiothreitol (DTT), 1% (v/v) protease cocktail inhibitor (Sigma, St Louis, MO, United States) and 0.5% (v/v) Triton X-100]. After taking aliquots for pigment analysis, the homogenate was centrifuged for 3 min at 16,800 g at 4°C (Sigma 2-16K, SIGMA Laborzentrifugen GmbH, Osterode am Harz, Germany) and the supernatant (crude extract) was kept at 4°C and immediately used for measuring the activities of Rubisco (EC 4.1.1.39) and PEPC (EC 4.1.1.31).

The activities of Rubisco were assayed at 25°C by $^{14}CO_2$ incorporation into acid-stable products according to Parry et al. (1997) to with modifications (Correia et al., 2020). The assay medium (1 mL per sample) contained 50 mM Bicine-KOH pH 8.2, 40 mM $MgCl_2$, 10 mM $NaH^{14}CO_3$ (7.4 kBq μM^{-1}) and 0.4 mM ribulose-1,5-bisphosphate (RuBP). To measure Rubisco initial activity (V_i), 25 μL of crude extract was added to assay medium, and the reaction stopped after 1 min with the addition of 100 μL of 1 M HCl. To determine Rubisco total activity (V_t), 25 μL of crude extract was added to assay medium without RuBP for 3 min, to allow the carbamylation of enzyme catalytic sites. Rubisco V_t reaction was started by adding RuBP and stopped after 1 min with the addition of 100 μL of 1 M HCl. The mixture was completely dried at 60°C after which the residue was resuspended in 0.5 mL of distilled water and mixed with 5 mL of scintillation liquid (BioSafe LS Cocktail, Beckman, United States). Radioactivity of the ^{14}C incorporated in the acid-stable products was measured by scintillation counting (LS 7800 spectrophotometer, Beckmann Instruments Inc., Fullerton, CA, United States). Rubisco activation state (%) was determined by the V_i/V_t ratio.

PEPC physiological ($V_{physiol}$) and maximum (V_{max}) activities were measured in a continuous assay at 340 nm and 25°C (UV500 UV-Visible spectrophotometer, Unicam, Cambridge, United Kingdom) according to Bakrim et al. (1992) with some modifications (Carmo-Silva et al., 2007). The reaction mixture for $V_{physiol}$ (1 mL) consisted of 50 mM HEPES-KOH pH 7.2, 10 mM $MgCl_2$, 10 mM $NaHCO_3$, 2.5 mM PEP (Sigma), 12 units of MDH (Sigma) and 20 μL of crude extract. For V_{max}, the reaction mixture consisted of 50 mM HEPES-KOH pH 8.0, 10 mM $MgCl_2$, 10 mM $NaHCO_3$, 10 mM PEP (Sigma), 12 units of MDH (Sigma) and 20 μL of extract. In both cases, the reaction was started by the addition of 0.2 mM (final concentration) NADH (Sigma). Each measured activity is the mean of three replicate on the same extract. PEPC activation state (%) was calculated as $V_{physiol}/V_{max}$ ratio.

For pigment analysis, each 20 μL aliquot previously retrieved from the leaf extract was diluted in 980 μL of methanol. After mixing in the vortex, the samples were left in the dark at 4°C overnight. After centrifuging for 1 min at 13,000 g at 4°C (Sigma 2-16K, SIGMA Laborzentrifugen GmbH, Osterode am Harz, Germany), the absorbance at 470, 652.4, 665.2, and 700 nm were measured in an Epoch™ 2 Microplate Spectrophotometer (BioTek, Winooski, VT, United States). Pigment concentrations were determined according to the equations in Lichtenthaler and Buschmann (2001).

Antioxidant Enzyme Assays

To extract the soluble protein fraction, leaf samples were grinded in a cooled mortar with 0.5 mL of 50 mM sodium/potassium phosphate extraction buffer (with 0.1 mM Na-EDTA, 2 mM PVP, 10 mM DTT, 0.1 mM PMSF, and 24 μM NADP, pH 7.6).

The homogenate was centrifuged at 13,000 g for 10 min at 4°C (Sigma 2-16K, SIGMA Laborzentrifugen GmbH, Osterode am Harz, Germany) and the supernatant was collected to a new tube. Protein concentration was determined according to Bradford (1976) in an Epoch^{TM} 2 Microplate Spectrophotometer (BioTek, Winooski, VT, United States).

Catalase (CAT; EC 1.11.1.6) activity was measured according to Teranishi et al. (1974), through H_2O_2 consumption monitoring and the decrease in absorbance at 240 nm (ε = 39.4 mM^{-1} cm^{-1}). The reaction mixture contained 50 mM of sodium/potassium phosphate buffer (pH 7.0), and 30 mM of H_2O_2 with the reaction being started by the addition of 5 μL of extract. Ascorbate peroxidase (APx; EC 1.11.1.11) was assayed according to Tiryakioglu et al. (2006). The reaction mixture contained 50 mM of sodium/potassium phosphate buffer (pH 7.0), 0.1 mM of H_2O_2, and 0.25 mM L-ascorbate, and the reaction was also initiated with the addition of 5 μL of the extract. The activity was recorded as the decrease in absorbance at 290 nm and the amount of ascorbate oxidized calculated from the molar extinction coefficient (ε = 2.8 mM^{-1} cm^{-1}). Guaiacol peroxidase (GOPx; EC 1.11.1.7) activity was assayed according to Mika and Lüthje (2003) through the monitorization of guaiacol oxidation at 470 nm (ε = 26.6 mM^{-1} cm^{-1}). The reaction mixture contained 50 mM of sodium/potassium phosphate buffer (pH 7.0), 10 mM of H_2O_2, and 8 mM guaiacol, and the reaction was initiated with the addition of 5 μL of the extract. Superoxide dismutase (SOD; EC 1.15.1.1) activity was assayed according to Marklund and Marklund (1974) by measuring the reduction of pyrogallol at 325 nm. The reaction mixture contained 30 mM of sodium/potassium phosphate buffer (pH 7.0) and 0.24 mM of pyrogallol, with the reaction being started by the addition of 5 μL of extract. Glutathione reductase (GR; EC 1.8.1.7) activity was assayed according to Edwards et al. (1990) by measuring the fall in absorbance at 340 nm as NADPH was oxidized (ε = 6.22 mM^{-1} cm^{-1}). The reaction mixture contained 25 mM of sodium/potassium phosphate extraction buffer (pH 7.6), 0.5 mM of oxidized glutathione and 0.2 mM NADPH, starting the reaction by the addition of 5 μL of extract. Control assays were done in the absence of substrate to evaluate the autoxidation of the substrates. All assays were performed in a total volume of 200 μL per well at 25°C in an Epoch^{TM} 2 Microplate Spectrophotometer (BioTek, Winooski, VT, United States).

Lipid Peroxidation Analysis

Lipid peroxidation products were determined as previously described (Heath and Packer, 1968). Leaves were homogenized briefly in 1.5 mL of 10% (v/v) trichloroacetic acid (TCA), containing 0.4% (w/v) thiobarbituric acid (TBA). The reaction was conducted at 100°C for 30 min, being halted through placement in ice. After centrifugation at 15,000 g for 10 min at 4°C (Sigma 2-16K, SIGMA Laborzentrifugen GmbH, Osterode am Harz, Germany), 1 mL of the supernatant was collected and mixed with 1 mL of 0.4% TBA and incubated again under the same conditions. The absorbance of the supernatant was recorded at 532 and 600 nm by spectrophotometry (UV500 UV-Visible Spectrometer, Unicam, Waltham, MA, United States). The concentration of malondialdehyde (MDA) was determined using the molar extinction coefficient (ε = 155 mM^{-1} cm^{-1}).

Fatty Acid Profiles

The analysis of fatty acid was performed by direct trans-esterification of leaf samples, in freshly prepared methanol sulphuric acid (97.5:2.5, v/v), at 70°C for 60 min, using the internal standard pentadecanoic acid (C15:0) (Feijão et al., 2018). Fatty acid methyl esters (FAME) were recovered using petroleum ether, dried with an N_2 flow, and re-suspended in an adequate amount of hexane. The FAME solution was analyzed through gas chromatography (Varian 430-GC gas chromatograph equipped with a hydrogen flame ionization detector set at 300°C, Middelburg, Netherlands), by addition of 1 μL, setting the injector temperature to 270°C, with a split ratio of 50. The fused-silica capillary column (50 m × 0.25 mm; WCOT Fused Silica, CP-Sil 88 for FAME; Varian, Middelburg, Netherlands) was maintained at a constant nitrogen flow of 2.0 mL min^{-1} and the oven set to 190°C. Fatty acids identification was performed by comparison of retention times with standards (Sigma-Aldrich) and chromatograms were analyzed by the peak surface method, using the Galaxy software. The double bond index (DBI) was calculated, to determine the membrane saturation levels, as previously described (Feijão et al., 2018):

$$DBI = \frac{2 \times (\%\ \text{monoenes} + 2 \times \%\ \text{dienes} + 3 \times \%\ \text{trienes})}{100} \quad (1)$$

Statistical Analysis

Since the data lacked normality and homogeneity, the statistical analysis was based on Mann-Whitney non-parametric tests (GraphPad Prism 8.4.2 for Windows, GraphPad Software, San Diego, CA, United States). Multivariate statistical analyses [SIMPER and Canonical Analysis of Principal Coordinates (CAP)] were performed using Primer 6 software (Clarke and Gorley, 2006). The data obtained from the Kautsky plots, thermography data, oxidative stress and fatty acids were used

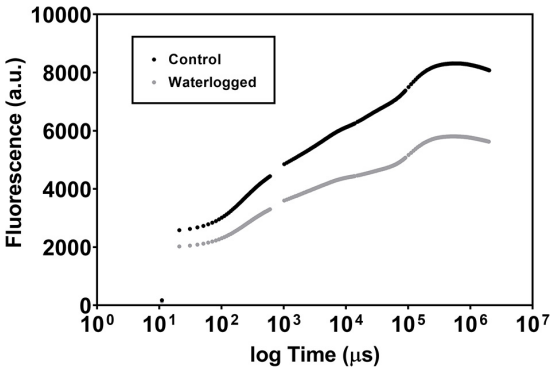

FIGURE 2 | Chlorophyll transient kinetics (Kautsky plots) in leaves of control plants (dark gray) and waterlogged plants (light gray) of *Spartina patens* after 30 days (mean ± s.d., *n* = 10).

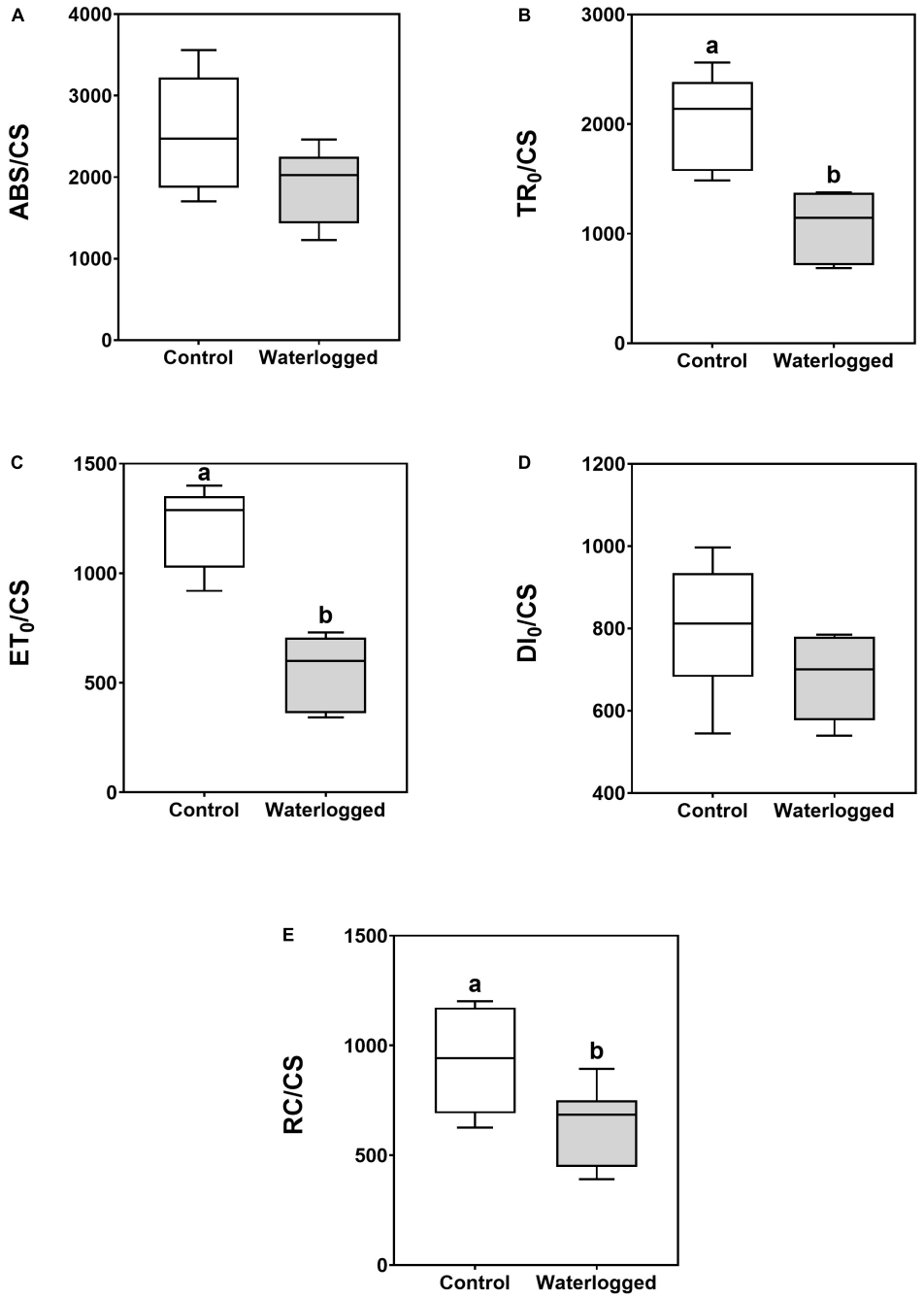

FIGURE 3 | Boxplots of leaf energy fluxes [**A**, absorbed (ABS/CS); **B**, trapped (TR_0/CS); **C**, transported (ET_0/CS); **D**, dissipated (DI_0/CS)] and **(E)** the number of available reaction centers per cross-section (RC/CS) in leaves of control plants (white boxes) and waterlogged plants (gray boxes) of *Spartina patens* after 30 days (n = 10, different letters indicate significant differences at $p < 0.05$).

as the basis for the construction of the respective resemblance matrixes based on the Euclidean distances between samples. To evaluate the different metabolic datasets obtained as a whole (in opposition to univariate analysis), statistical multivariate models based on Kautsky plots, thermography data, oxidative stress and fatty acids were generated using Principal Coordinates Analysis (PCO) (Clarke and Gorley, 2006).

RESULTS

Chlorophyll *a* PAM Analysis

Observing the Kautsky plots resultant from the *in vivo* PAM fluorometric analysis, lower fluorescence values could be observed in plants subjected to the treatment when compared with control plants (**Figure 2**).

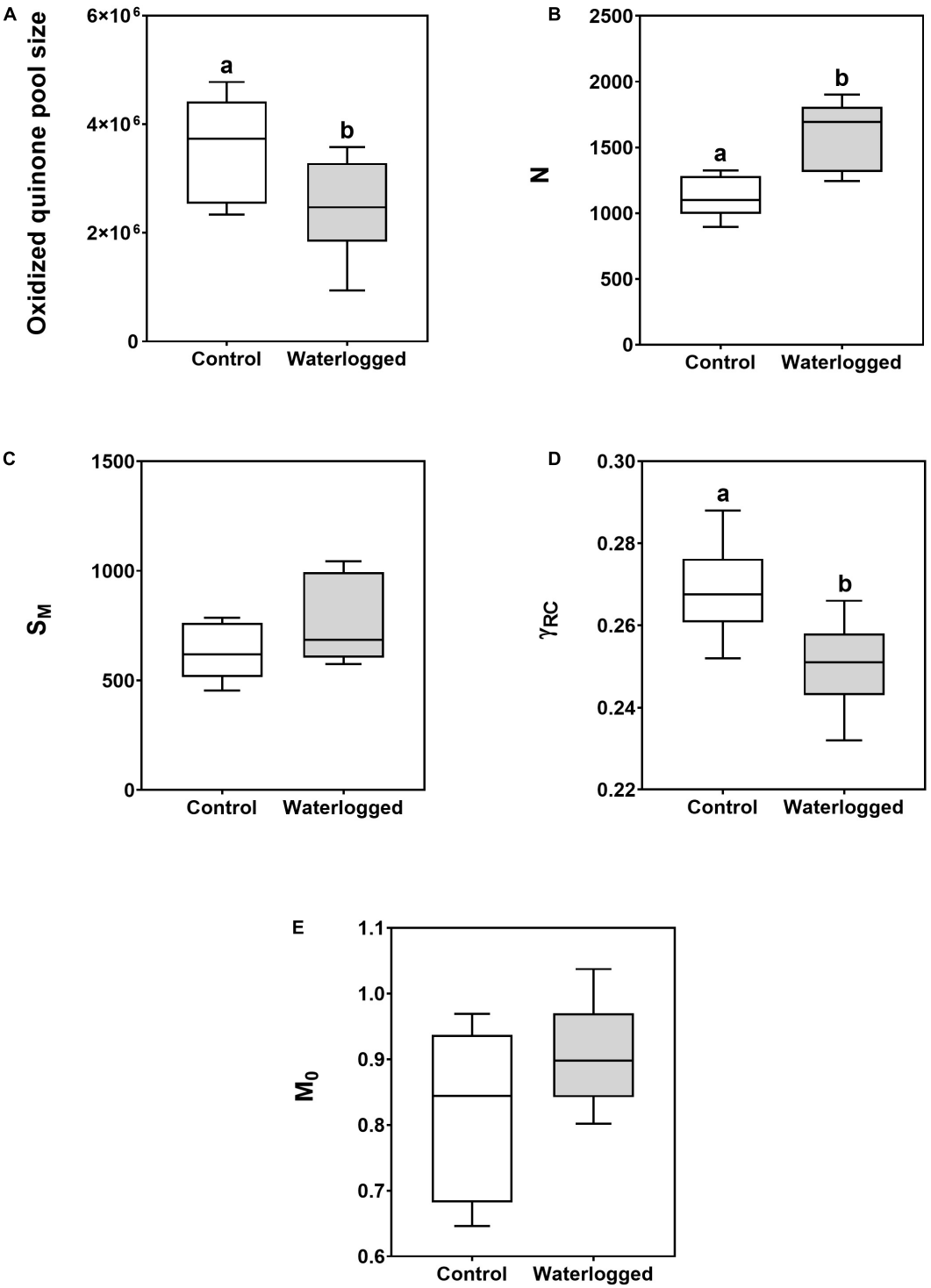

FIGURE 4 | Boxplots of the photosystem II and ETC related photochemical traits [**A**, oxidized quinone pool; **B**, reaction center turnover rate (N); **C**, the energy needed to close all reaction centers (S_M); **D**, the probability that a PSII chlorophyll molecule function as a RC (γ_{RC}); **E**, net rate of PS II RC closure (M_0)], in leaves of control plants (white boxes) and waterlogged plants (gray boxes) of *Spartina patens* after 30 days ($n = 10$, different letters indicate significant differences at $p < 0.05$).

The four energy fluxes [**Figure 3**: A, energy absorbed by the photosystem II (PS II) antennae (ABS/CS); B, energy trapped inside the PS II (TR_0/CS); C, energy transported within the electron transport chain (ETC) (ET_0/CS); and D, the energy dissipation flux (DI_0/CS)] showed the same pattern presenting lower values in the

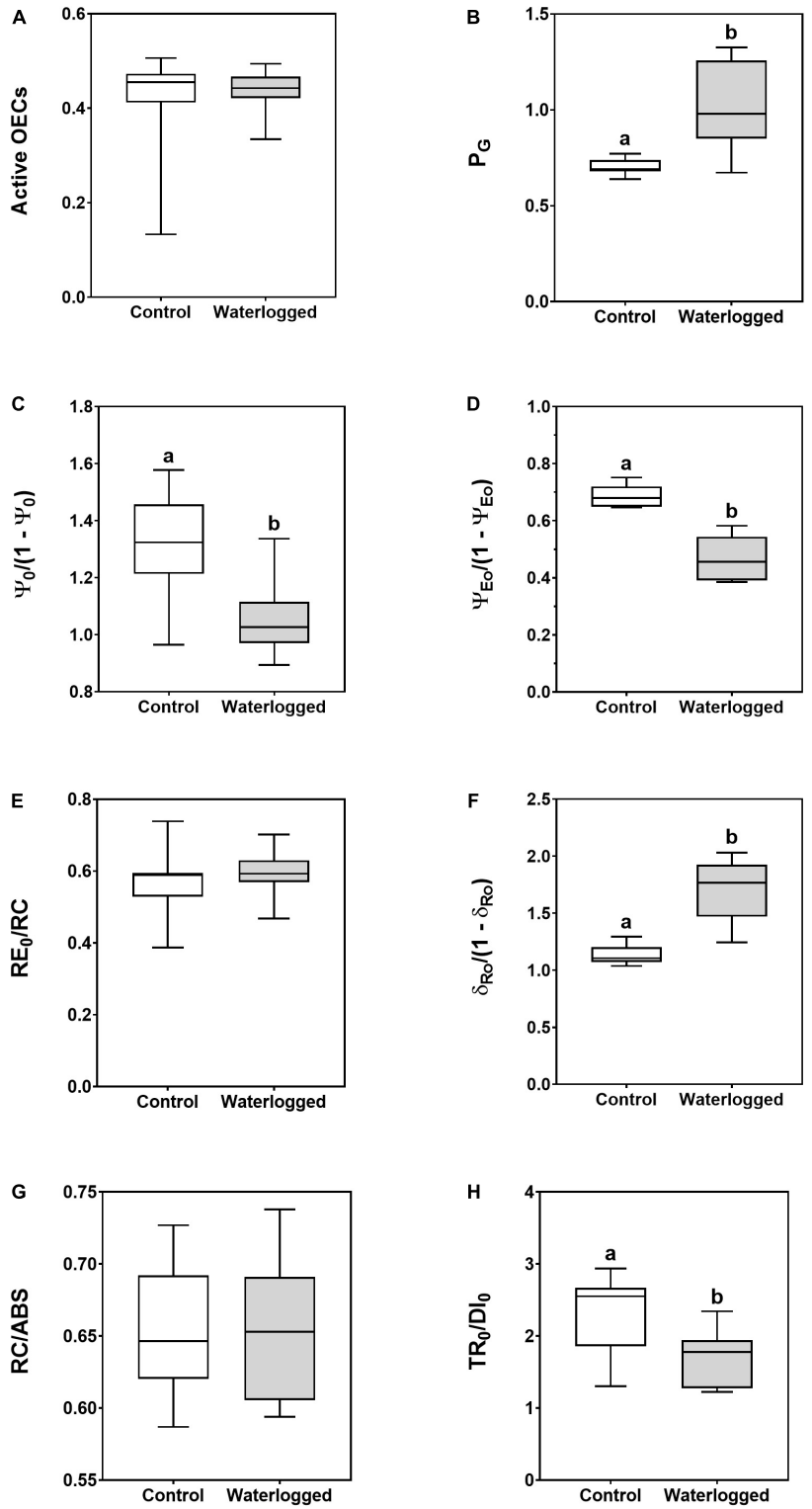

FIGURE 5 | Boxplots of the photosystems I (PS I) and II (PS II) photochemical traits. **(A)** Active oxygen-evolving complexes (OECs); **(B)** grouping probability between the two PS II units (PG); **(C)** the contribution of the dark reactions from quinone A to plastoquinone [$\psi_0/(1 - \psi_0)$]; **(D)** the equilibrium constant for the redox reactions between PS II and PS I [$\psi_{E0}/(1 - \psi_{E0})$]; **(E)** electron transport from PQH_2 to the reduction of PS I end electron acceptors (RE_0/RC); **(F)** the contribution of PS I reducing its end acceptors [$\delta_{R0}/(1- \delta_{R0})$]; **(G)** reaction center II density within the antenna chlorophyll bed of PS II (RC/ABS); **(H)** contribution or partial performance due to the light reactions for primary photochemistry (TR_0/DI_0), in leaves of control plants (white boxes) and waterlogged plants (gray boxes) of *Spartina patens* after 30 days ($n = 10$, different letters indicate significant differences at $p < 0.05$).

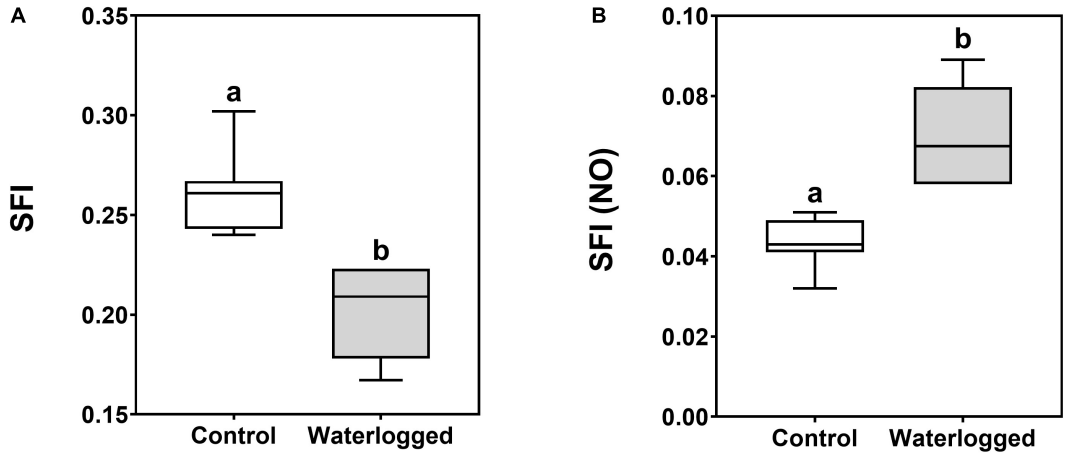

FIGURE 6 | Boxplots of the structure functional indexes for photosynthesis (**A**, SFI) and non-photosynthetic or dissipation processes [**B**, SFI (NO)] in leaves of control plants (white boxes) and waterlogged plants (gray boxes) of *Spartina patens* after 30 days (n = 10, different letters indicate significant differences at $p < 0.05$).

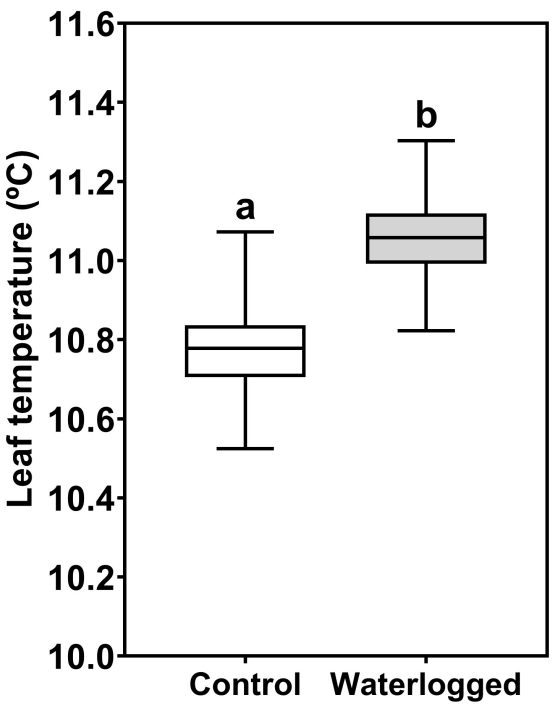

FIGURE 7 | Boxplots of the leaf surface temperature measured through infrared thermography in leaves of control plants (white box) and waterlogged plants (gray box) of *Spartina patens* after 30 days (n = 10, different letters indicate significant differences at $p < 0.05$).

waterlogged plants, although that decrease was only statistically significant for TR_0/CS and ET_0/CS. It was also a similar reduction in the number of oxidized PS II reaction centers (RC/CS) (**Figure 3E**).

Further analysis of the functioning of different components of the photosystems and ETC (**Figure 4**) showed a decrease in the oxidized quinone pool size in the waterlogged plants, followed by an enhancement in the number of QA redox turnovers until maximum fluorescence was reached (N). Although no significant changes were observed in the energy needed to close all RCs (S_M), there was a decrease in the probability of a PS II chlorophyll molecule functioning as a RC (γ_{RC}) in the treated plants. However, no significant differences were observed in the QA reduction rate (M_0).

Although the active oxygen-evolving complexes (OEC) showed no differences between control and waterlogged plants (**Figure 5A**), the P_G, the grouping probability that correlates with the disconnection between the two PS II units, increased in the later plant group (**Figure 5B**).

Regarding PS II and PS I, waterlogged plants presented a significant decrease in photochemical processes, both in the contribution of light (TR_0/DI_0; **Figure 5H**) and dark [$\psi_0/(1 - \psi_0)$; **Figure 5C**] reactions of the photochemical cycle. On the other hand, at the PS I level there was a significant increase in the activity of this photosystem [$\delta_{R0}/(1 - \delta_{R0})$; **Figure 5F**] in the intervened plants, although there was a decrease in the equilibrium constant for the redox reaction between both photosystems toward the PS II [$\psi_{E0}/(1 - \psi_{E0})$; **Figure 5D**]. Nevertheless, there were no significant changes in the reaction center density within the PS II antenna chlorophyll bed (RC/ABS; **Figure 5G**) or in the electron transport from PQH_2 to the reduction of the PS I end acceptors (RE_0/RC; **Figure 5E**).

In summary and observing the structure functional indexes, there was a decrease of the photochemical processes (**Figure 6A**) and an increase of the non-photochemical or dissipative processes (**Figure 6B**) in the waterlogged plants.

Leaf Thermography

Regarding leaf surface temperature measured through infrared thermography, there was a statistically significant increase in temperature in the treated plants (11.06°C) relatively to control ones (10.77°C) (**Figure 7**).

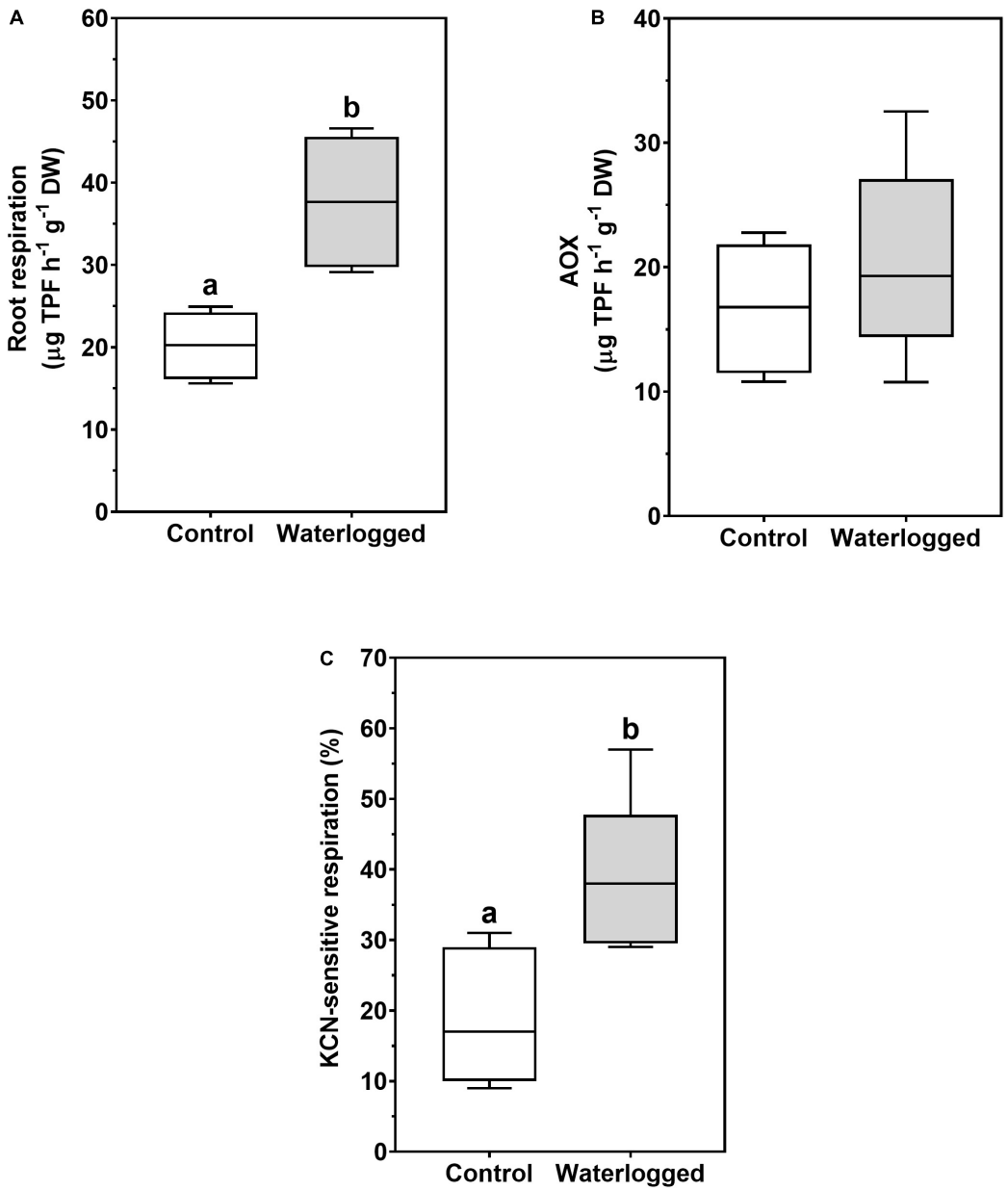

FIGURE 8 | Boxplots of root respiration **(A)**, alternative oxidase (AOX) activity **(B)**, and percentage of KCN-sensitive respiration **(C)** in roots of control plants (white boxes) and waterlogged plants (gray boxes) of *Spartina patens* after 30 days ($n = 5$, different letters indicate significant differences at $p < 0.05$).

Root Respiration

An increase of root respiration in waterlogged plants was measured (**Figure 8A**), resulting not from changes in the alternative oxidase (AOX) activity (**Figure 8B**) but rather from a twofold increase in KCN-sensitive respiration (**Figure 8C**).

Proline

Leaves of waterlogged plants of *S. patens* experienced a fivefold increase in proline (**Figure 9**), to *circa* 20 μmol g^{-1} FW, contrasting with the leaves of control plants with *circa* 4 μmol g^{-1}.

C4-Photosynthetic Carboxylating Enzymes and Pigment Analysis

Relatively to the C4-photosynthetic carboxylating enzymes activities, no statistically significant changes were observed either in the activation state, or maximal (V_{max}) and physiological ($V_{physiol}$) rates of PEPC (**Supplementary Figure 1**), or the activation state, or initial (V_i) and total (V_t) rates of Rubisco (**Supplementary Figure 2**). The same was observed for pigments Chl *a*, Chl *b*, total chlorophyll, and carotenoids (**Supplementary Figure 3**).

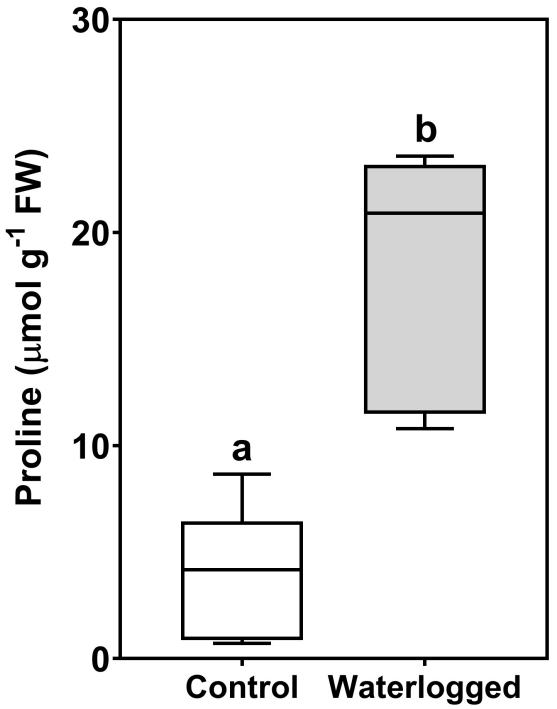

FIGURE 9 | Boxplots of proline content in leaves of control plants (white box) and waterlogged plants (gray box) of *Spartina patens* after 30 days ($n = 5$, different letters indicate significant differences at $p < 0.05$).

Antioxidant Enzyme Analysis

Regarding the antioxidant enzymes CAT, APx, GOPx, SOD, and GR (**Figure 10**), only the latter two showed a significant decrease in activity on waterlogged plants, with a decrease of twofold in SOD and almost a threefold in GR.

Lipid Peroxidation and Fatty Acid Profile

While lipid peroxidation products increased in waterlogged plants (**Figure 11A**), no changes occurred in total fatty acids content (**Figure 11B**).

Regarding the relative abundance of fatty acids, there was a decrease in triunsaturated hexadecatrienoic acid (16:3), exclusively present in plastidial lipids, whilst there was an increase in stearic acid (C18:0) of waterlogged plants relative to controls (**Figure 12**). Although there were no significant changes in the major fatty acids classes (**Supplementary Figure 4**), the ratio of saturated to unsaturated fatty acids ratio (SFA/UFA) increased in waterlogged plants (**Supplementary Figure 5**).

Biophysical and Biochemical Profiles

The multivariate PCO analysis allowed to distinguish the control from the waterlogged plants of *S. patens* using the Kautsky plot, leaf thermography, oxidative stress data and fatty acid profiles (**Figures 13**, **14**), which explain the variables' total variation with various degrees. Through the simple application of remote tools (**Figure 13**), the Kautsky plot first PCO axis explains 98.9% of the whole variation between the two evaluated groups (**Figure 13A**), while due to a higher dispersion along the second PCO axis, the thermography data PCO1 has a lower explanatory power (64.8% of total variation) (**Figure 13B**).

Observing the biochemical profiles, the oxidative stress measurements reveal good separation of the two groups (87.3% of total variation), along only one axis of the PCO (**Figure 14A**). On the other hand, when evaluating the samples fatty acid profiles, it was possible to observe a dispersion along the two PCO axis, indicative of a higher dispersion in the biochemical characteristics of the samples and lower explanatory power (46.2% of total variation) (**Figure 14B**).

DISCUSSION

The impacts of a highly aggressive and invasive species, such as *S. patens* urges the need to develop measures, to counteract its spreading. Control measures should be directed to this species and are less harmful to the surrounding environment and co-occurring species. Our proposed alternative method for eliminating the invasive halophyte *S. patens* proved to be a very effective method to significantly increase the stress levels of the plants in 30 days, using the species physiology drawbacks. Results provide new insights for an ecoengineering solution to be applied in future *S. patens* control measures in intertidal systems. The fact that *S. patens* do not tolerate waterlogging is the only limiting factor that is currently preventing full occupation of the intertidal border (Burdick, 1989; Bertness, 1991; Curado et al., 2020), and fully replacing other halophyte native species. Furthermore, once the NIS is removed, indigenous species, such as *H. portulacoides* and *S. fruticosa* can reoccupy that area and restore habitat functionality (Curado et al., 2020). Thus, any tool that facilitates this NIS dieback, is of added value to recover the ecosystem floristic diversity.

The effect of waterlogging on *S. patens* was very clear in different photochemical-related variables and showed lower photosynthetic efficiency when compared with the non-intervened plants, although no significant changes were observed in C4 photosynthesis-related enzymes PEPC and Rubisco as well as in the pigment profile.

The observation of the two distinct treatments of *S. patens* showed a depression in the Kautsky curves of the waterlogged plants, presenting lower fluorescence values, a characteristic of stress effects (Duarte et al., 2015). Energy fluxes suffered a major impact at the level of electron transport (ET_0/CS), with a reduction in the quinone pool size, given by the area above the transient curve (Strasser et al., 1995; Joliot and Joliot, 2002), and a decrease in the number of available reaction centers (RC/CS). This leads to an excessive energy accumulation (Kalaji et al., 2011) that can destroy the D1 protein, and eventually impair all photochemical machinery (Demmig-Adams and Adams, 1992; Qiu et al., 2003; Duarte et al., 2013). To prevent oxidative damage in the chloroplasts, this high energy accumulation needs to be dissipated, frequently through the xanthophyll cycle (Demmig-Adams and Adams, 1992). However, no changes were observed in the carotenoid pool, occurring a decrease in photochemical

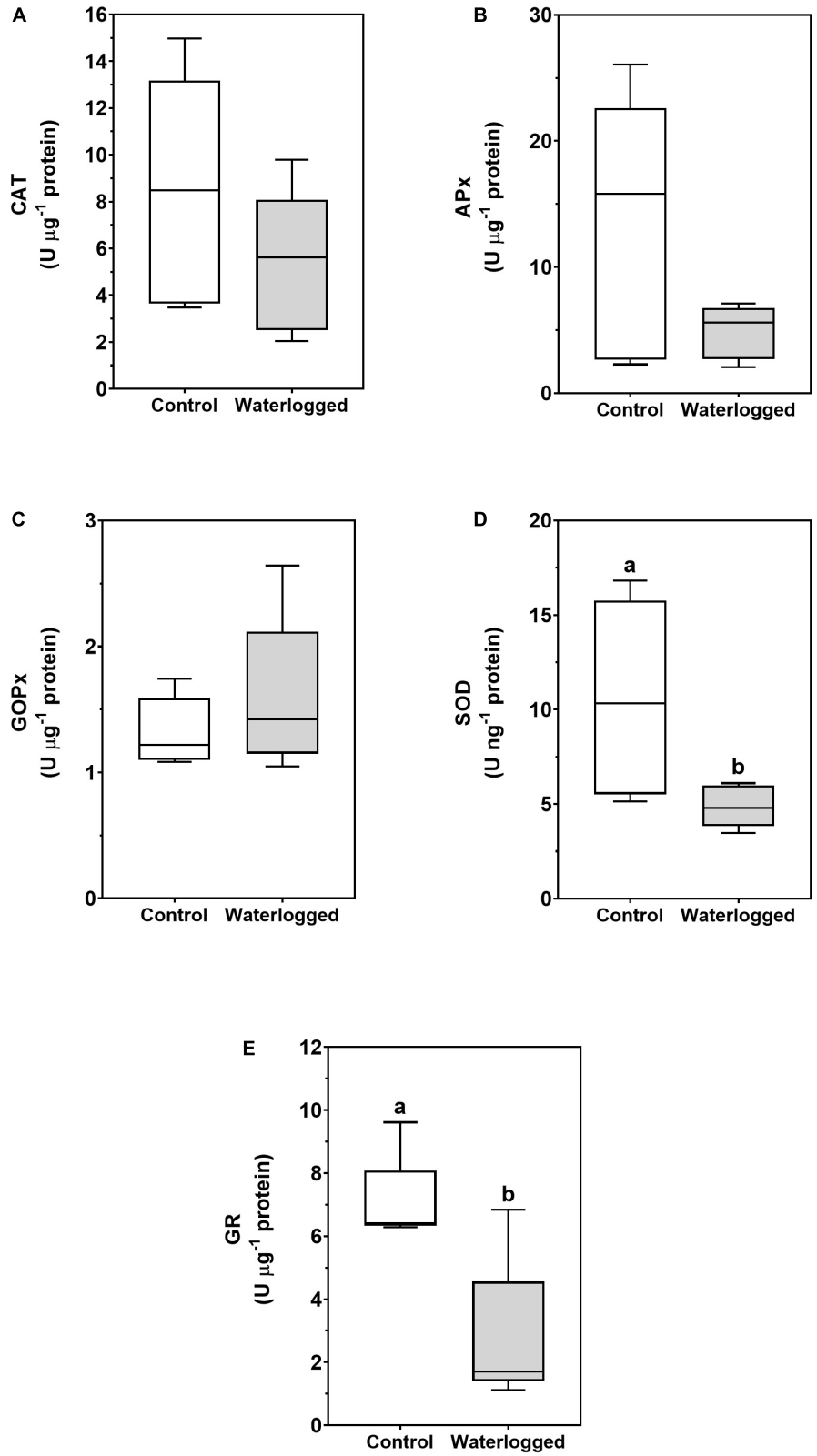

FIGURE 10 | Boxplots of catalase (CAT, **A**), ascorbate peroxidase (APX, **B**), guaiacol peroxidase (GOPx, **C**), superoxide dismutase (SOD, **D**) and glutathione reductase (GR, **E**) enzymatic activities in leaves of control plants (white boxes) and waterlogged plants (gray boxes) of *Spartina patens* after 30 days ($n = 5$, different letters indicate significant differences at $p < 0.05$).

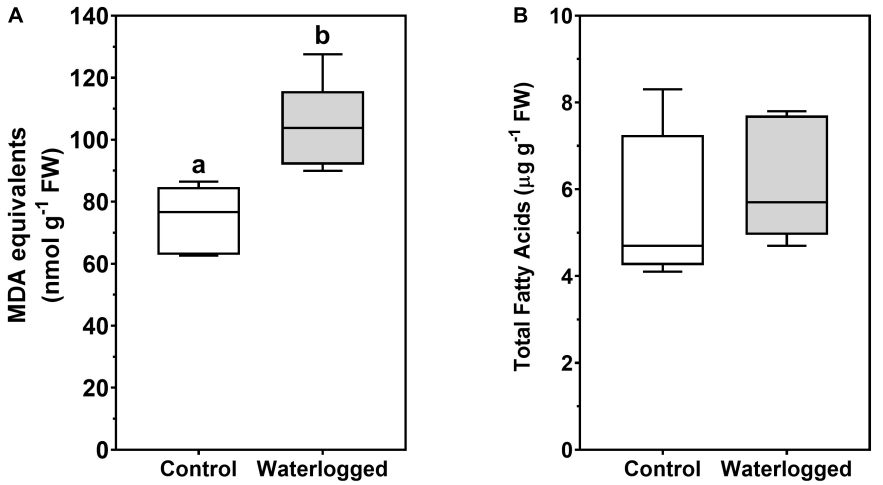

FIGURE 11 | Boxplots of lipid peroxidation quantification measured as malondialdehyde (MDA) equivalents **(A)** and total fatty acid content **(B)** in leaves of control plants (white boxes) and waterlogged plants (gray boxes) of *Spartina patens* after 30 days ($n = 5$, different letters indicate significant differences at $p < 0.05$).

quenching and an increase in non-photochemical quenching (NPQ), leading to a decrease in the lumen pH, attributed to protonation of the light-harvesting complexes (LHC) proteins associated with the PSII (Cousins et al., 2002). This, in turn, can explain the increase in leaf temperature observed in the waterlogged plants (Zhang et al., 2019). Moreover, it was possible to observe that waterlogged plants had their trapped and transported energy fluxes reduced, but no increase in the energy dissipation. Under stress, a common feature observed is a maintenance of the absorbed and trapped energy flux, but a low energy use in the electron transport, leading to energy bursts inside the chloroplast that are normally diverted to dissipation in the form of heat or fluorescence (Duarte et al., 2016). In this case, only a reduction of the trapped and energy transport fluxes indicating a lower ability of the plants to harvest light, a condition that can promote leaf senescence and plant mortality.

With the roots under water for a more prolonged time, it would be expected to observe a decrease in root respiration (Pan et al., 2021). However, *S. patens* can develop aerenchyma, pumping atmospheric oxygen through the leaves to ventilate the roots and, thus, allowing it to increase its respiration (Burdick and Mendelssohn, 1987; Burdick, 1989). Nevertheless, and considering the lower energy harvested by waterlogged plants, increased root respiration and consequent consumption of energy reserves (such as carbohydrates), will inevitably increase the energetic stress of the plants. *Spartina patens* also presented an increased proline content in its leaves, increasing leaf water potential to counteract the differential osmotic pressures between soil and leaves (Briens and Larher, 1982; Koyro et al., 2006; Aziz et al., 2011). This mechanism also poses significant energetic costs to the individuals, that while trying to counteract the waterlogging osmotic constraints, end up increasing the degree of energetic stress of the plants (Iqbal et al., 2014).

Oxygen deprivation will lead inevitably to the increase of intracellular reactive oxygen species (ROS) due to metabolism impairment under stress (Bailey-Serres and Chang, 2005; Pucciariello et al., 2012), severely damaging, amongst others, proteins, and lipids of cells membranes (Sharma et al., 2012; Baxter et al., 2014). Nevertheless, under waterlogging no increase in the antioxidant enzymatic activity could be observed, thus contributing to the accumulation of ROS inside the cells of the waterlogged plants. In fact, two first-line defense enzymes (SOD and GR) had their activities severely reduced. All these impairments of the antioxidant enzymatic system are concomitant with the observed increase in lipid peroxidation. Once again, this will impose severe energetic stress, due to damage in the membranes of the energetic organelles and thus impacting the electronic transport systems and the cell energy budgets.

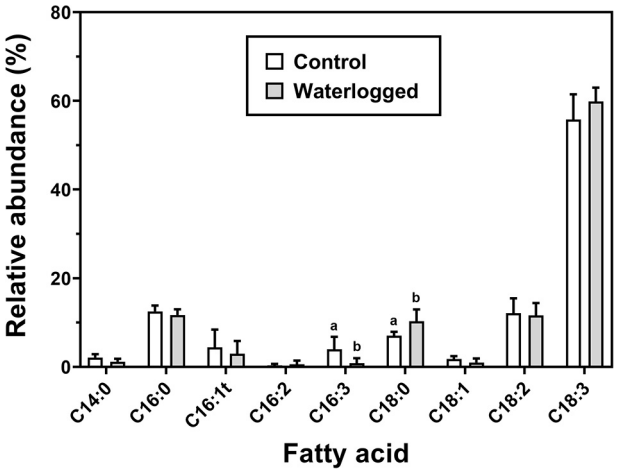

FIGURE 12 | Fatty acid profile in leaves of control plants (white boxes) and waterlogged plants (gray boxes) of *Spartina patens* after 30 days ($n = 5$, different letters indicate significant differences at $p < 0.05$).

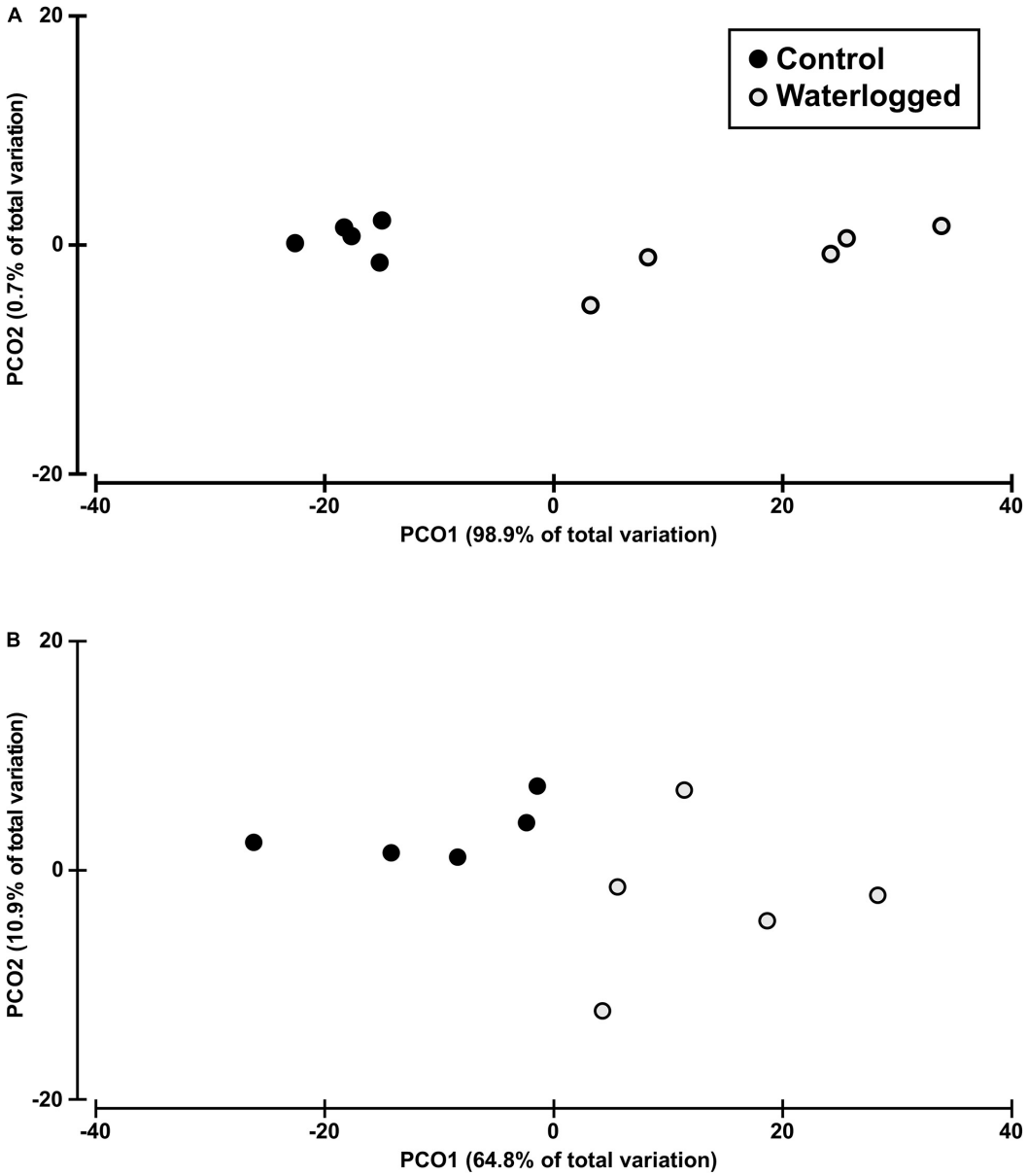

FIGURE 13 | Canonical analysis plot based on the Kautsky plot **(A)**, and thermography **(B)** in leaves of control plants (black circles) and waterlogged plants (gray circles) of *Spartina patens* after 30 days ($n = 5$, different letters indicate significant differences at $p < 0.05$).

Additionally, exposure to waterlogging also induced changes in the fatty acid profile of *S. patens*, which increased the ratio between saturated and unsaturated fatty acids, mainly contributed by an increase in stearic acid (C18:0), which likely resulted in a decrease in membrane fluidity. Moreover, there was a significant decrease in the triunsaturated hexadecatrienoic acid (16:3), which is present in the major plastidial lipid monogalactosyldiacylglycerol and can be linked to lower photosynthetic efficiency measured in waterlogged plants (Kobayashi et al., 2016).

Using multivariate analysis of the assessed biophysical and biochemical traits it was possible to observe that techniques, such as PAM and infrared thermography, are the most efficient tools to evaluate *in situ* the success of the intervention and the stress levels imposed on the plants targeted to be removed. As in previous ecological studies in response to stress (Cruz de Carvalho et al., 2020a,b; Duarte et al., 2020), the use of bio-optical techniques (e.g., Kautsky plot) allowed an efficient identification of the waterlogged plants and, thus, provide efficient and reliable tools to monitor the success of control interventions, without disturbing the process itself and allowing repeated measures over the intervention period.

In terms, of the ecoengineering solution tested in the present work, the physiological changes observed indicate that

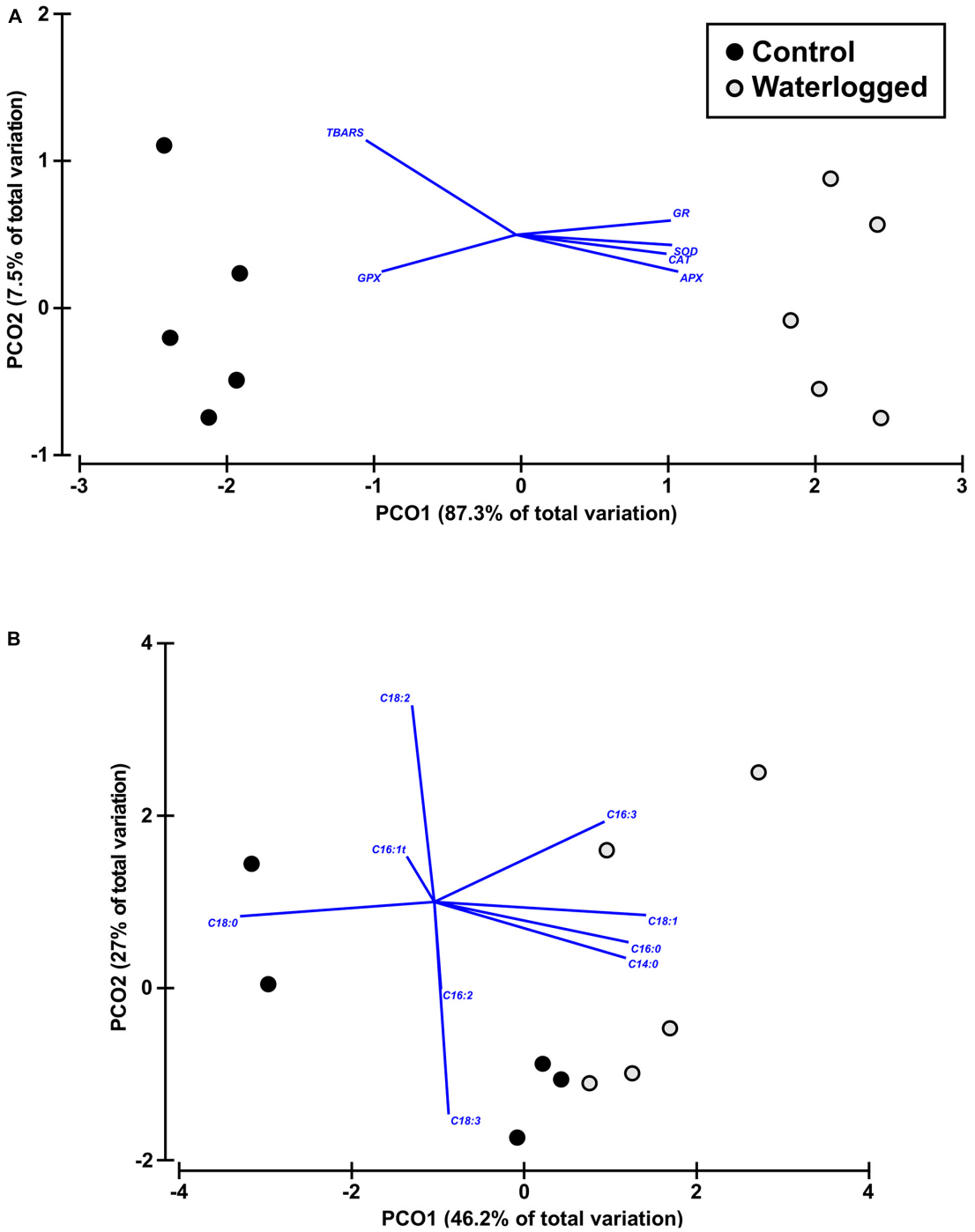

FIGURE 14 | Canonical analysis plot based on oxidative stress (antioxidant enzymes and lipid peroxidation) data **(A)**, and fatty acid profile **(B)** in leaves of control plants (black circles) and waterlogged plants (gray circles) of *Spartina patens* after 30 days ($n = 5$, different letters indicate significant differences at $p < 0.05$).

the adopted strategy can be an eco-friendly control measure, increasing the plants stress levels significantly, although in the considered 30-day period there was no plant mortality, indicating that these control measures should be performed in more prolonged periods.

CONCLUSION

The application of a simple barrier to allow waterlogging proved to be an effective and low-cost solution to impair the physiology and biochemical pathways of the invasive halophyte

S. patens. Although long-term studies need to be performed, this ecoengineering solution has the potential to control and eliminate this species from salt marshes and other intertidal systems in future ecosystem restoration programs. Since *S. patens* turfs are easily identified, the upscaling of this technique could involve the application of tubes with different diameters according to plant turfs density, allowing waterlogging to be prolonged in space and time. Furthermore, the application of a simple bio-optical tool will allow the stakeholders to easily follow the process of suppressing the species without the interference of the process and allowing repeated measures over the intervention period.

DATA AVAILABILITY STATEMENT

The raw data supporting the conclusions of this article will be made available by the authors, without undue reservation.

AUTHOR CONTRIBUTIONS

BD, VF, and PR-S: conceptualization. BD: methodology, supervision, project administration, and funding acquisition. RC and BD: formal analysis. RC, EF, ID, VP, MS, AS, and AM: investigation. RC: data curation and writing—original draft preparation. EF, ID, VP, MS, AM, AS, IC, PR-S, VF, and BD: writing—review and editing. All authors have read and agreed to the published version of the manuscript.

FUNDING

BD and VF were supported by investigation contracts (CEECIND/00511/2017 and DL57/2016/CP1479/CT0024). PR-S was supported by FCT through a postdoctoral grant (SFRH/BPD/95784/2013). We would like to thank the Fundação para a Ciência e a Tecnologia (FCT) for funding the research *via* project grants PTDC/CTA-AMB/30056/2017 (OPTOX), UID/MAR/04292/2019, and UIDB/04046/2020. We would also like to thank the MAR2020 program through the project RESTAURA2020 (16-01-04-FMP-0014).

SUPPLEMENTARY MATERIAL

The Supplementary Material for this article can be found online at: https://www.frontiersin.org/articles/10.3389/fmars.2021.699528/full#supplementary-material

REFERENCES

Aguiar, F. C. F., and Ferreira, M. T. (2013). Plant invasions in the rivers of the Iberian Peninsula, south-western Europe: A review. *Plant Biol.* 147, 1107–1119. doi: 10.1080/11263504.2013.861539

Ainouche, M., and Gray, A. (2016). Invasive Spartina: lessons and challenges. *Biol. Invas.* 18, 2119–2122. doi: 10.1007/s10530-016-1201-7

Aziz, I., Gul, B., Gulzar, S., and Ajmal Khan, M. (2011). Seasonal variations in plant water status of four desert halophytes from semi-arid region of Karachi. *Pak. J. Bot.* 43, 587–594.

Bailey-Serres, J., and Chang, R. (2005). Sensing and signalling in response to oxygen deprivation in plants and other organisms. *Ann. Bot.* 96, 507–518. doi: 10.1093/aob/mci206

Bakrim, N., Echevarria, C., Cretin, C., Arrio-Dupont, M., Pierre, J. N., Vidal, J., et al. (1992). Regulatory phosphorylation of Sorghum leaf phosphoenolpyruvate carboxylase. Identification of the protein-serine kinase and some elements of the signal-transduction cascade. *Eur. J. Biochem.* 204, 821–830. doi: 10.1111/j.1432-1033.1992.tb16701.x

Bates, L. S., Waldren, R. P., and Teare, I. D. (1973). Rapid determination of free proline for water-stress studies. *Plant Soil* 39, 205–207. doi: 10.1007/BF00018060

Baumel, A., Rousseau-Gueutin, M., Sapienza-Bianchi, C., Gareil, A., Duong, N., Rousseau, H., et al. (2016). Spartina versicolor Fabre: Another case of Spartina trans-Atlantic introduction? *Biol. Invasions* 18, 2123–2135. doi: 10.1007/s10530-016-1128-z

Baxter, A., Mittler, R., and Suzuki, N. (2014). ROS as key players in plant stress signalling. *J. Exp. Bot.* 65, 1229–1240. doi: 10.1093/jxb/ert375

Bertness, M. D. (1991). Zonation of Spartina patens and Spartina alterniflora in New England Salt Marsh. *Ecology* 72, 138–148. doi: 10.2307/1938909

Bradford, M. M. (1976). A rapid and sensitive method for the quantitation of microgram quantities of protein utilizing the principle of protein-dye binding. *Anal. Biochem.* 72, 248–254. doi: 10.1016/0003-2697(76)90527-3

Briens, M., and Larher, F. (1982). Osmoregulation in halophytic higher plants: a comparative study of soluble carbohydrates, polyols, betaines and free proline. *Plant Cell Environ.* 5, 287–292. doi: 10.1111/1365-3040.ep11572682

Brunner, I., Brodbeck, S., and Walthert, L. (2002). Fine root chemistry, starch concentration, and "vitality" of subalpine conifer forests in relation to soil pH. *For. Ecol. Manage* 165, 75–84. doi: 10.1016/S0378-1127(01)00633-8

Burdick, D. M. (1989). Root aerenchyma development in Spartina patens in response to flooding. *Am. J. Bot.* 76, 777–780. doi: 10.2307/2444425

Burdick, D. M., and Mendelssohn, I. A. (1987). Waterlogging responses in dune, swale and marsh populations of Spartina patens under field conditions. *Oecologia* 74, 321–329. doi: 10.1007/BF00378924

Caçador, I., Neto, J. M., Duarte, B., Barroso, D. V., Pinto, M., and Marques, J. C. (2013). Development of an Angiosperm Quality Assessment Index (AQuA-Index) for ecological quality evaluation of Portuguese water bodies - A multi-metric approach. *Ecol. Indic.* 25, 141–148. doi: 10.1016/j.ecolind.2012.09.021

Carmo-Silva, A. E., Powers, S. J., Keys, A. J., Arrabaça, M. C., and Parry, M. A. J. (2008). Photorespiration in C4 grasses remains slow under drought conditions. *Plant Cell Environ.* 31, 925–940. doi: 10.1111/j.1365-3040.2008.01805.x

Carmo-Silva, A. E., Soares, A. S., Marques, da Silva, J., Bernardes da Silva, A., Keys, A. J., et al. (2007). Photosynthetic responses of three C4 grasses of different metabolic subtypes to water deficit. *Funct. Plant Biol.* 34, 204–213. doi: 10.1071/FP06278

Clarke, K. R., and Gorley, R. N. (2006). *PRIMER v6: User Manual/Tutorial*. England: Plymouth.

Correia, P. M. P., Silva, A. B., Roitsch, T., Carmo−Silva, E., and Marques da Silva, J. (2020). Photoprotection and optimization of sucrose usage contribute to faster recovery of photosynthesis after water deficit at high temperatures in wheat. *Physiol. Plant* 2020:13227. doi: 10.1111/ppl.13227

Cousins, A. B., Adam, N. R., Wall, G. W., Kimball, B. A., Pinter, P. J., Ottman, M. J., et al. (2002). Photosystem II energy use, non-photochemical quenching and the xanthophyll cycle in Sorghum bicolor grown under drought and free-air CO2 enrichment (FACE) conditions. *Plant. Cell Environ.* 25, 1551–1559. doi: 10.1046/j.1365-3040.2002.00935.x

Couto, T., Duarte, B., Barroso, D., Caçador, I., and Marques, J. C. (2013). Halophytes as sources of metals in estuarine systems with low levels of contamination. *Function. Plant Biol.* 2013, 931–939. doi: 10.1071/FP12300

Cruz de Carvalho, R., Feijão, E., Kletschkus, E., Marques, J. C., Reis-Santos, P., Fonseca, V. F., et al. (2020a). Halophyte bio-optical phenotyping: A multivariate

photochemical pressure index (Multi-PPI) to classify salt marsh anthropogenic pressures levels. *Ecol. Indic.* 119:106816. doi: 10.1016/j.ecolind.2020.106816

Cruz de Carvalho, R., Feijão, E., Matos, A. R., Cabrita, M. T., Novais, S. C., Lemos, M. F. L., et al. (2020b). Glyphosate-Based Herbicide Toxicophenomics in Marine Diatoms: Impacts on Primary Production and Physiological Fitness. *Appl. Sci.* 10:10217391. doi: 10.3390/app10217391

Curado, G., Gallego-Tévar, B., Figueroa, E., and Castillo, J. M. (2020). Effects of removal of alien Spartina densiflora and restoration of native S. maritima on succession and zonation in European salt marshes. *Estuar. Coast. Shelf Sci.* 244:105815. doi: 10.1016/j.ecss.2018.04.011

Demmig-Adams, B., and Adams, W. W. (1992). *Photoprotection and other responses of plants to high light stress*. Available online at: www.annualreviews.org (accessed April 23, 2021).

Duarte, B., Baeta, A., Rousseau-Gueutin, M., Ainouche, M., Marques, J. C., and Caçador, I. (2015). A tale of two spartinas: Climatic, photobiological and isotopic insights on the fitness of non-indigenous versus native species. *Estuar. Coast. Shelf Sci.* 167, 178–190. doi: 10.1016/j.ecss.2015.06.015

Duarte, B., Carreiras, J., and Caçador, I. (2021). Climate Change Impacts on Salt Marsh Blue Carbon, Nitrogen and Phosphorous Stocks and Ecosystem Services. *Appl. Sci.* 11, 1–18. doi: 10.3390/app11041969

Duarte, B., Couto, T., Freitas, J., Valentim, J., Silva, H., Marques, J. C., et al. (2013). Abiotic modulation of Spartina maritima photobiology in different latitudinal populations. *Estuar. Coast. Shelf Sci.* 130, 127–137. doi: 10.1016/j.ecss.2013.02.008

Duarte, B., Feijão, E., Cruz de Carvalho, R., Duarte, I. A., Silva, M., Matos, A. R., et al. (2020). Effects of Propranolol on Growth, Lipids and Energy Metabolism and Oxidative Stress Response of Phaeodactylum tricornutum. *Biology* 9:478. doi: 10.3390/biology9120478

Duarte, B., Marques, J. C., and Caçador, I. (2016). Ecophysiological response of native and invasive *Spartina species* to extreme temperature events in Mediterranean marshes. *Biol. Invasions* 18, 2189–2205. doi: 10.1007/s10530-015-0958-4

Duarte, B., Pedro, S. S., Marques, J. C., Adão, H., and Caçador, I. (2017). Zostera noltii development probing using chlorophyll a transient analysis ({JIP}-test) under field conditions: Integrating physiological insights into a photochemical stress index. *Ecol. Indic.* 76, 219–229. doi: 10.1016/j.ecolind.2017.01.023

Duarte, C. M., Poiner, I., and Gunn, J. (2018). Perspectives on a Global Observing System to Assess Ocean Health. *Front. Mar. Sci.* 5:265. doi: 10.3389/fmars.2018.00265

Edwards, E. A., Rawsthorne, S., and Mullineaux, P. M. (1990). Subcellular distribution of multiple forms of glutathione reductase in leaves of pea (Pisum sativum L.). *Planta* 180, 278–284. doi: 10.1007/BF00194008

EU (2020). *Communication from the Commission to the European Parliament, the Council, the European Economic and Social Committee and the Committee of the Regions - EU Biodiversity Strategy for 2030*. Available online at: https://eur-lex.europa.eu/legal-content/EN/TXT/HTML/?uri=CELEX:52020DC0380&from=EN. (accessed April 16, 2021).

Feijão, E., Gameiro, C., Franzitta, M., Duarte, B., Caçador, I., Cabrita, M. T., et al. (2018). Heat wave impacts on the model diatom Phaeodactylum tricornutum: Searching for photochemical and fatty acid biomarkers of thermal stress. *Ecol. Indic.* 95, 1026–1037. doi: 10.1016/j.ecolind.2017.07.058

Heath, R. L., and Packer, L. (1968). Photoperoxidation in isolated chloroplasts. I. Kinetics and stoichiometry of fatty acid peroxidation. *Arch. Biochem. Biophys.* 125, 189–198. doi: 10.1016/0003-9861(68)90654-1

Hedge, P., Kriwoken, L., and Patten, K. (2003). A Review of Spartina Management in Washington State. *US. J. Aquat. Plant Manag.* 41, 82–90.

Heywood, V. (1989). "Patterns, extents and modes of invasions by terrestrial plants," in *Biological invasions: a global perspective*, eds M. Drake, J. A. Mooney, H. A. di Castri, F. Groves, R. H. Kruger, F. J. Rejmanek, et al. (Chichester: John Wiley), 31–60.

Hultén, E. (1958). *he amphi-atlantic plants and their phytogeographical connections*. Stockholm: Almquist & Wiksell.

Iqbal, N., Umar, S., and Nazar, R. (2014). "Manipulating Osmolytes for Breeding Salinity-Tolerant Plants," in *Emerging Technologies and Management of Crop Stress Tolerance*, (Amsterdam: Elsevier Inc.), 385–404. doi: 10.1016/B978-0-12-800875-1.00016-8

Joliot, P., and Joliot, A. (2002). Cyclic electron transfer in plant leaf. *Proc. Natl. Acad. Sci. U. S. A.* 99, 10209–10214. doi: 10.1073/pnas.102306999

Kalaji, H. M., Bosa, K., and Ko, J. (2011). Effects of salt stress on photosystem II efficiency and CO 2 assimilation of two Syrian barley landraces. *Environ. Exp. Bot.* 73, 64–72. doi: 10.1016/j.envexpbot.2010.10.009

Kerr, D. W., Hogle, I. B., Ort, B. S., and Thornton, W. J. (2016). A review of 15 years of Spartina management in the San Francisco Estuary. *Biol. Invasions* 18, 2247–2266. doi: 10.1007/s10530-016-1178-2

Kobayashi, K., Endo, K., and Wada, H. (2016). "Roles of Lipids in Photosynthesis," in *Lipids in Plant and Algae Development*, eds Y. Nakamura and Y. Li-Beisson (Cham: Springer International Publishing), 21–49. doi: 10.1007/978-3-319-25979-6_2

Koyro, H.-W., Geissler, N., Hussin, S., and Huchzermeyer, B. (2006). *Mechanisms Of Cash Crop Halophytes To Maintain Yields And Reclaim Saline Soils In Arid Areas in Ecophysiology of High Salinity Tolerant Plants*. Netherlands: Springer, 345–366. doi: 10.1007/1-4020-4018-0_22

Lichtenthaler, H. K., and Buschmann, C. (2001). Chlorophylls and Carotenoids: Measurement and Characterization by UV-VIS Spectroscopy. *Curr. Protoc. Food Anal. Chem.* 1, 1–.4. doi: 10.1002/0471142913.faf0403s01

Major, W., Grue, C., Grassley, J., and Conquest, L. (2003). Mechanical and Chemical Control of Smooth Cordgrass in Waillapa Bay, Washington. *J. Aquat. Plant Manag.* 41, 6–12.

Marklund, S., and Marklund, G. (1974). Involvement of the Superoxide Anion Radical in the Autoxidation of Pyrogallol and a Convenient Assay for Superoxide Dismutase. *Eur. J. Biochem.* 47, 469–474. doi: 10.1111/j.1432-1033.1974.tb03714.x

Martínez-Jauregui, M., Soliño, M., Martínez-Fernández, J., and Touza, J. (2018). Managing the Early Warning Systems of Invasive Species of Plants, Birds, and Mammals in Natural and Planted Pine Forests. *Forests* 9:9040170. doi: 10.3390/f9040170

Mika, A., and Lüthje, S. (2003). Properties of Guaiacol Peroxidase Activities Isolated from Corn Root Plasma Membranes. *Plant Physiol.* 132, 1489L–1498. doi: 10.1104/pp.103.020396

Pan, J., Sharif, R., Xu, X., and Chen, X. (2021). Mechanisms of Waterlogging Tolerance in Plants: Research Progress and Prospects. *Front. Plant Sci.* 11:2319. doi: 10.3389/fpls.2020.627331

Parry, M. A. J., Andralojc, P. J., Parmar, S., Keys, A. J., Habash, D., Paul, M. J., et al. (1997). Regulation of Rubisco by inhibitors in the light. *Plant Cell Environ.* 20, 528–534. doi: 10.1046/j.1365-3040.1997.d01-85.x

Patten, K., O'Casey, C., and Metzger, C. (2017). Large-Scale Chemical Control of Smooth Cordgrass (Spartina alterniflora) in Willapa Bay, WA: Towards Eradication and Ecological Restoration. *Invasive Plant Sci. Manag.* 10, 284–292. doi: 10.1017/inp.2017.25

Pérez-Romero, J. A., Idaszkin, Y. L., Duarte, B., Baeta, A., Marques, J. C., Redondo-Gómez, S., et al. (2018). Atmospheric CO2 enrichment effect on the Cu-tolerance of the C4 cordgrass Spartina densiflora. *J. Plant Physiol.* 220, 155–166. doi: 10.1016/j.jplph.2017.11.005

Pucciariello, C., Parlanti, S., Banti, V., Novi, G., and Perata, P. (2012). Reactive oxygen species-driven transcription in Arabidopsis under oxygen deprivation. *Plant Physiol.* 159, 184–196. doi: 10.1104/pp.111.191122

Qiu, N., Lu, Q., and Lu, C. (2003). Photosynthesis, photosystem II efficiency and the xanthophyll cycle in the salt−adapted halophyte *Atriplex centralasiatica*. *New Phytol.* 159, 479–486. doi: 10.1046/j.1469-8137.2003.00825.x

Repolho, T., Duarte, B., Dionísio, G., Paula, J. R., Lopes, A. R., Rosa, I. C., et al. (2017). Seagrass ecophysiological performance under ocean warming and acidification. *Sci. Rep.* 7:41443. doi: 10.1038/srep41443

Ruf, M., and Brunner, I. (2003). Vitality of tree fine roots: reevaluation of the tetrazolium test. *Tree Physiol.* 23, 257–263. doi: 10.1093/treephys/23.4.257

Sharma, P., Jha, A. B., Dubey, R. S., and Pessarakli, M. (2012). Reactive Oxygen Species, Oxidative Damage, and Antioxidative Defense Mechanism in Plants under Stressful Conditions. *J. Bot.* 2012:217037. doi: 10.1155/2012/217037

Strasser, R. J., Srivastava, A., and Govindjee. (1995). Polyphasic Chlorophyll a Fluorescence Transient in Plants and Cyanobacteria. *Photochem. Photobiol.* 61, 32–42. doi: 10.1111/j.1751-1097.1995.tb09240.x

Teixeira, A., Duarte, B., and Caçador, I. (2014). "Salt Marshes and Biodiversity," in *Sabkha Ecosystems: Volume IV: Cash Crop Halophyte and Biodiversity Conservation*, eds M. A. Khan, B. Böer, M. Öztürk, T. Z. Al Abdessalaam, M.

Clüsener-Godt, and B. Gul (Dordrecht: Springer), 283–298. doi: 10.1007/978-94-007-7411-7_20

Teranishi, Y., Tanaka, A., Osumi, M., and Fukui, S. (1974). Catalase activities of hydrocarbon-utilizing candida yeasts. *Agric. Biol. Chem.* 38, 1213–1220. doi: 10.1080/00021369.1974.10861301

Tiryakioglu, M., Eker, S., Ozkutlu, F., Husted, S., and Cakmak, I. (2006). Antioxidant defense system and cadmium uptake in barley genotypes differing in cadmium tolerance. *J. Trace Elem. Med. Biol.* 20, 181–189. doi: 10.1016/j.jtemb.2005.12.004

☼UN (2020). *UN Decade on Ecosystem Restoration*. Available online at: https://www.decadeonrestoration.org/. (accessed April 16, 2021).

von Caemmerer, S. (2020). Rubisco carboxylase/oxygenase: From the enzyme to the globe: A gas exchange perspective. *J. Plant Physiol.* 252:153240. doi: 10.1016/j.jplph.2020.153240

Zhang, R., Zhou, Y., Yue, Z., Chen, X., Cao, X., Ai, X., et al. (2019). The leaf-air temperature difference reflects the variation in water status and photosynthesis of sorghum under waterlogged conditions. *PLoS One* 14:e0219209. doi: 10.1371/journal.pone.0219209

Conflict of Interest: The authors declare that the research was conducted in the absence of any commercial or financial relationships that could be construed as a potential conflict of interest.

Publisher's Note: All claims expressed in this article are solely those of the authors and do not necessarily represent those of their affiliated organizations, or those of the publisher, the editors and the reviewers. Any product that may be evaluated in this article, or claim that may be made by its manufacturer, is not guaranteed or endorsed by the publisher.